

Design of Surface Permanent Magnet Synchronous Motor Using Design Assist System for PMSM

Kenta Yamano* Student Member,
Masayuki Sanada* Senior Member,

Shigeo Morimoto^{*a)} Senior Member
Yukinori Inoue* Member

(Manuscript received Jan. 16, 2017, revised March 30, 2017)

Permanent magnet synchronous motors (PMSMs) possess many good characteristics, such as high efficiency and high torque density. In this study, a design assist system is proposed for PMSMs. This system uses motor parameters and a magnetic equivalent circuit to design a PMSM that satisfies the demanded output characteristics. This paper describes the outline of the design assist system. The system is applied to the design of surface permanent magnet synchronous motors (SPMSMs) and the effectiveness of the proposed system is confirmed.

Keywords: SPMSM, motor parameters, magnetic circuit, permeance model

1. Introduction

Permanent magnet synchronous motors (PMSMs) are widely used in many applications, such as home applications and electric vehicles. Due to their high efficiency and power density, they contribute to energy savings⁽¹⁾⁽²⁾.

An optimized motor design must take into account requirements such as the torque-speed characteristics and motor size, because they are different for each application⁽³⁾⁽⁴⁾. The PMSM design is complex, so engineers must have experience that designed a lot of various motors. However, the motor design typically involves time-consuming trial and errors^{(5)–(7)}. Therefore, a design assist system that can automatically decide the motor structure to decrease the trial and error process of the PMSM design is in demand.

This study proposes a design assist system for PMSM that automatically decides motor structures based on the demanded operating points on output characteristics and required motor size. The proposed system is applied to the design of surface permanent magnet synchronous motor (SPMSM), and two designed models are analyzed by the finite element method (FEM). The effectiveness of the proposed system is discussed by evaluating the results of the analyses.

2. Design Assist System for PMSM

A flowchart for the proposed design assist system is shown in Fig. 1. The proposed system determines the motor structure parameters from the motor parameters obtained from the demanded operating points on output characteristics and the restriction of motor size.

The system is divided into two processes: (1) selection of the motor parameters and (2) calculation of the motor

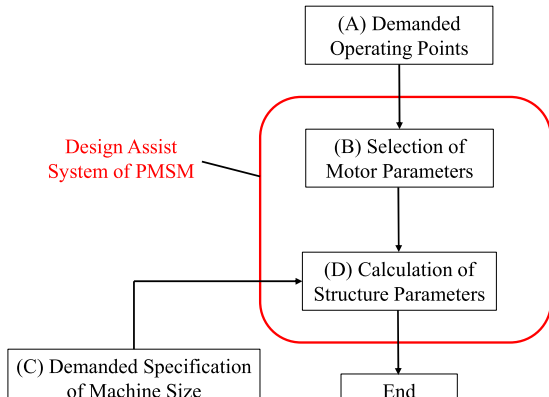


Fig. 1. Flowchart for proposed design assist system

structure parameters. First, the motor parameters satisfying the demanded operating points are selected with consideration of the optimal current vector control under the current and voltage limitations. Then, the magnetic equivalent circuit based on the permeance model is used in the calculation of the motor structure parameters by using the motor parameters.

Each process is described in detail in the following.

3. Selection of Motor Parameters

The voltage equation and the torque of a surface permanent magnet synchronous motor (SPMSM) modeled in the *d*-*q* reference frame are expressed as follows:

$$\begin{bmatrix} v_d \\ v_q \end{bmatrix} = \begin{bmatrix} R_a + pL_a & -\omega L_a \\ \omega L_a & R_a + pL_a \end{bmatrix} \begin{bmatrix} i_d \\ i_q \end{bmatrix} + \begin{bmatrix} 0 \\ \omega \Psi_a \end{bmatrix} \dots\dots (1)$$

$$T = P_n \Psi_a i_q \dots\dots (2)$$

where

v_d, v_q *d*- and *q*-axis voltages
 i_d, i_q *d*- and *q*-axis currents
 R_a armature resistance

a) Correspondence to: Shigeo Morimoto. E-mail: morimoto@eis.osakafu-u.ac.jp

* Osaka Prefecture University
1-1, Gakuencho, Naka-ku, Sakai, Osaka 591-8531, Japan

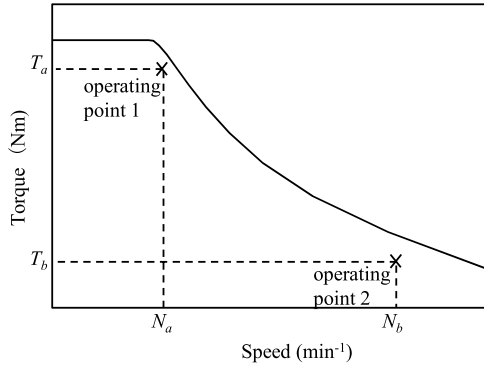


Fig. 2. Example of torque vs. speed characteristics

L_a	inductance (corresponding to d - and q -axis inductances L_d , L_q)
ω	electrical rotor angular velocity
p	differential operator
P_n	number of pole pairs

Equations (1) and (2) show that the output characteristics of the SPMSM depend on the motor parameters. Motor parameters are important in the SPMSM design because they decide the torque vs. speed characteristics like Fig. 2. In the proposed design assist system of the SPMSM, motor parameters satisfying the demanded operating points on output characteristics are found and used to design the SPMSM. To find the motor parameters satisfying the demanded output characteristics, this system uses the optimal current vector control method to obtain the maximum output under the current and voltage limitations.

The current and voltage are limited to

$$V_o = \omega \sqrt{(\Psi_a + L_a i_d)^2 + (L_a i_q)^2} \leq V_{om} \quad (3)$$

$$I_a = \sqrt{i_d^2 + i_q^2} \leq I_{am} \quad (4)$$

where

V_o	induced voltage
V_{om}	induced voltage limit
I_a	armature current
I_{am}	armature current limit

In the following, the relationships between the motor parameters and the demanded operating points like Fig. 2 are derived under the current vector control methods.

3.1 Maximum Torque per Ampere Control Maximum torque per ampere (MTPA) control is applied in the region of speed where the induced voltage V_o does not exceed the induced voltage limit V_{om} . In this control region, the armature current I_a is equal to the current limit I_{am} , and the induced voltage V_o is less than the voltage limit V_{om} . The d - and q -axis currents in the control region and torque are given as follows:

$$i_{d1} = 0 \quad (5)$$

$$i_{q1} = I_{am} \quad (6)$$

$$T = P_n \Psi_a I_{am} \quad (7)$$

From (7), the magnet flux-linkage Ψ_a is calculated as follows:

$$\Psi_a = \frac{T}{P_n I_{am}} \quad (8)$$

From (8) and the demanded maximum torque T_a in Fig. 2, the relationship between Ψ_a and L_a satisfying the demanded maximum torque is obtained.

3.2 Base Speed When the induced voltage V_o reaches the voltage limit V_{om} under maximum torque per ampere control, the speed is called base speed ω_{base} . From (3), (5) and (6), the base speed for SPMSM is given as follows:

$$\omega_{base} = \frac{V_{om}}{\sqrt{\Psi_a^2 + (L_a I_{am})^2}} \quad (9)$$

From (9), the relationship between the motor parameters of L_a and Ψ_a is as follows:

$$L_a = \frac{1}{I_{am}} \sqrt{\left(\frac{V_{om}}{\omega_{base}}\right)^2 - \Psi_a^2} \quad (10)$$

From (10) and base speed N_{base} ($= N_a$) in Fig. 2, the relationship between Ψ_a and L_a satisfying the demanded base speed is obtained.

3.3 Flux-weakening Control for Maximizing Torque

Induced voltage increases with increasing rotor speed. When the motor speed reaches the base speed under MTPA control, the induced voltage becomes equal to the induced voltage limit. Therefore, the induced voltage V_o is controlled to the induced voltage limit V_{om} by flux-weakening (FW) control above the base speed. In this control region, voltage and current are equal to their limiting values. The d - and q -axis currents in this control region are given as follows:

$$i_{d2} = \frac{\left(\frac{V_{om}}{\omega}\right)^2 - \Psi_a^2 - L_d^2 I_{am}^2}{2L_a \Psi_a} \quad (11)$$

$$i_{q2} = \sqrt{I_{am}^2 - i_{d2}^2} \quad (12)$$

From (2), (11) and (12), the relationship between the motor parameters is as follows:

$$L_a = \frac{P_n \sqrt{A(\Psi_a^2 + B^2) - 2(T^2 + \sqrt{C - D})}}{A} \quad (13)$$

where

$$A = P_n^2 I_{am}^2$$

$$B = V_{om}/\omega$$

$$C = (T^2 + AB\Psi_a)^2$$

$$D = AT^2(B + \Psi_a)^2$$

From (13) and the torque and speed at the demanded high speed operating point, such as operating point 2 (T_b and N_b) in Fig. 2, the relationship between Ψ_a and L_a satisfying the demanded operating point is obtained.

3.4 Maximum Torque per Voltage Control

If Ψ_{dmin} ($= \Psi_a - L_a I_{am}$) < 0 , maximum torque can be obtained in the high-speed flux-weakening region by applying maximum torque per voltage (MTPV) control. In this control region, induced voltage V_o is equal to voltage limit V_{om} and armature current I_a is less than current limit I_{am} . The d - and q -axis currents in this control region are given as follows:

$$i_{d3} = -\frac{\Psi_a}{L_a} \quad (14)$$

$$i_{q3} = \frac{V_{om}}{\omega L_a} \quad (15)$$

Table 1. Operating points and electrical specification

Item (Unit)		Value
Operating point 1	Speed N_a (min ⁻¹)	1500
	Torque T_a (Nm)	10
Operating point 2	Speed N_b (min ⁻¹)	3000
	Torque T_b (Nm)	5
Armature current limit I_{am} (A)		20
Induced voltage limit V_{om} (V)		100
Voltage limit of inverter V_{lim} (V)		160

From (2), (14) and (15), the relationship between motor parameters is as follows:

$$L_a = \frac{P_n V_{om} \Psi_a}{\omega T} \dots \dots \dots (16)$$

From (16) and torque and speed like T_b and N_b in Fig. 2, the relationship between Ψ_a and L_a satisfying the demanded operating point is obtained.

3.5 Voltage Limit of Inverter The SPMSM is usually driven by an inverter. In the high speed region, the induced voltage V_o is controlled under the induced voltage limit V_{om} by flux-weakening control. However, the back electromotive force due to the permanent magnet can no longer be controlled when the uncontrolled generator mode occurs as a result of inverter shutdown at high speeds. To drive the SPMSM safely, the induced voltage under the no-load state must not exceed the voltage limit of inverter V_{lim} . The voltage limit V_{lim} corresponds to the voltage on the d - q coordinate converted from the withstand voltage of the inverter (limit value of the DC link voltage) which is determined by the withstand voltage of power device and the breakdown voltage of the smoothing capacitor. In the proposed system, it is considered that no-load induced voltage doesn't exceed V_{lim} . This condition is expressed as follows:

$$V_{lim} = \omega \Psi_a \dots \dots \dots (17)$$

From (17), magnet flux-linkage Ψ_a is as follows:

$$\Psi_a = \frac{V_{lim}}{\omega} \dots \dots \dots (18)$$

From (18) and maximum operating speed like N_b in Fig. 2, the maximum value of Ψ_a satisfying the voltage limit of the inverter is obtained.

3.6 Design of Motor Parameters The demanded operating points and limiting values discussed in this paper are shown in Table 1. In this paper, the voltage limit of inverter V_{lim} was set to 160 V as shown in Table 1. Generally, the induced voltage limit V_{om} determined by the DC link voltage during normal operation is set lower than V_{lim} in consideration of the safety factor, so it was set to 100 V in this paper.

In the design of the SPMSM, motor parameters satisfying two demanded operating points under the limitations of current and voltage are obtained from (8), (10), (13), (16), (18) and Table 1. The motor parameters region is shown in Fig. 3. In Fig. 3, border 1 is obtained from (8) and T_a in Table 1. The right side of border 1 shows the motor parameters satisfying the maximum torque T_a . Border 2 is obtained from (10) and N_a in Table 1. The lower side of border 2 shows

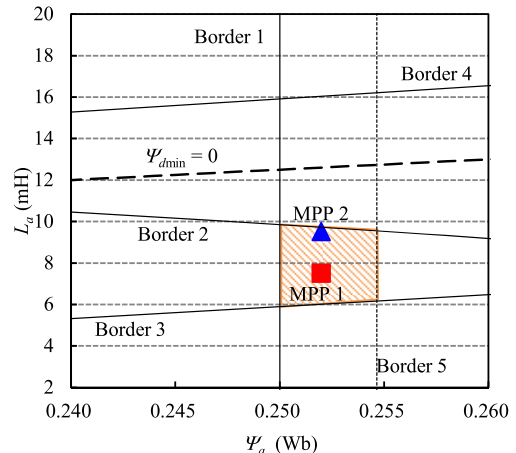


Fig. 3. Motor parameters region

Table 2. Values of MPP 1 and MPP 2

Item (Unit)	Value	
Selected motor parameters	MPP 1	MPP 2
Magnet flux-linkage Ψ_a (Wb)	0.252	0.252
Inductance L_a (mH)	7.5	9.5

the motor parameters satisfying the base speed of N_a . Border 3 is obtained from (13) and T_b and N_b in Table 1. The upper side of border 3 shows the motor parameters satisfying T_b and N_b . Border 4 is obtained from (16) and T_b and N_b in Table 1. The lower side of border 4 shows the motor parameters satisfying T_b and N_b . Finally, border 5 is obtained from (18) and N_b in Table 1. The left side of border 5 shows the motor parameters satisfying the voltage limit of the inverter at N_b . Therefore, the motor parameters satisfying the conditions listed in Table 1 exist within the region enclosed by borders 1, 2, 3, 4 and 5, which correspond to the hatched area in Fig. 3. This area can be theoretically obtained based on the theory described in 3.1 to 3.5 without the experience or skill of the designer.

In this design, motor parameter points 1 and 2 (MPP 1, MPP 2) in Fig. 3 are selected. The values of MPP 1 and 2 are shown in Table 2. If the motor parameters near each border was selected, the margin for the demanded operating points decreases. In consideration of margin, MPP 1 was selected as the design point near the center of the hatched area in Fig. 3. On the other hand, it is known that the decrease of torque at high speed becomes small when the combination of motor parameters close to the line representing $\Psi_{dmin} = 0$ are selected. The motor parameter point MPP 2 was selected to confirm that.

The torque versus speed characteristics calculated by using the motor parameters at MPP 1 and 2 are shown in Fig. 4. Figure 4 shows that SPMSMs with motor parameters selected by Fig. 3 satisfy the demanded operating points 1 and 2 shown in Table 1. Therefore, the motor parameters at MPP 1 and 2 are used for the design of SPMSMs that satisfy the demanded specifications of Table 1. Figure 4 also shows that the torque at high speed for MPP2 is larger.

4. Calculation of Motor Structure Parameters

The diagram of the calculation of the motor structure

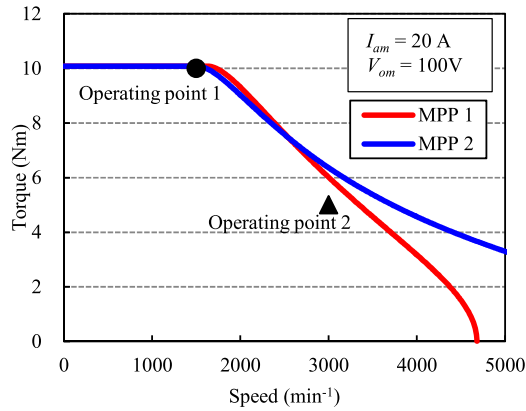


Fig. 4. Torque vs. speed characteristics calculated using motor parameters at MPP 1 and 2

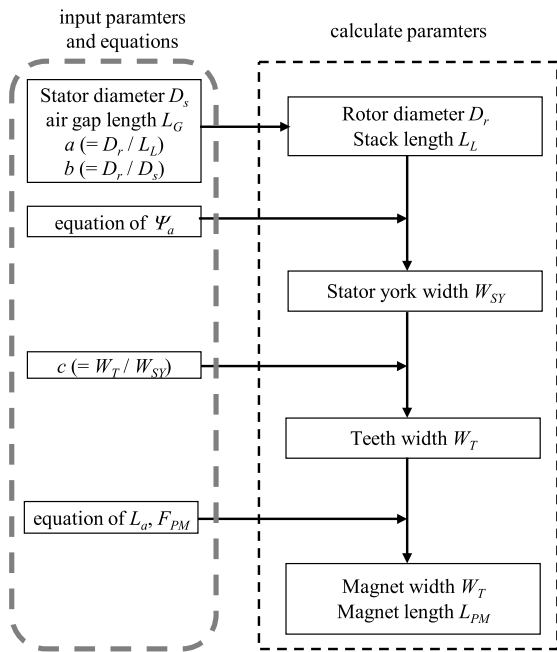


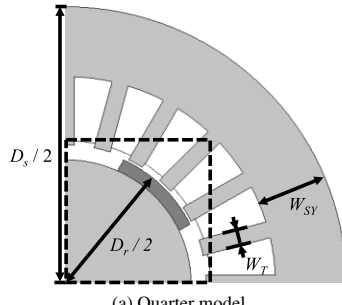
Fig. 5. Method of SPMSM design

parameters is shown in Fig. 5. In this method, motor structure parameters are obtained from motor parameters such as Ψ_a and L_a . To obtain the motor structure parameters from motor parameters, this system uses a simple magnetic equivalent circuit based on the permeance model.

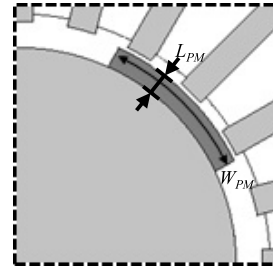
4.1 Permeance Model An example of the design model and the motor structure parameters is shown in Fig. 6. The model is SPMSM which is a four-pole SPMSM with distributed winding stator with 24 slots. Using the design system, D_r , L_I , $W_{S\bar{Y}}$, W_T , L_{PM} and W_{PM} are calculated.

The magnetic equivalent circuit considered in this system is shown in Fig. 7 and a list of reluctances is shown in Table 3. In Fig. 7, the numbers of reluctances and motor structure parameters are set as small as possible in order to calculate the structure parameters. In the following, relationship between the motor structure parameters and the motor parameters is shown using the magnetic equivalent circuit.

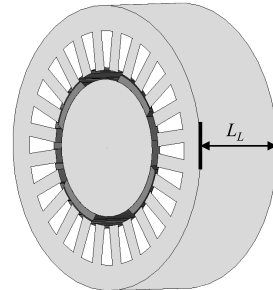
4.2 Magnet Flux-Linkage Magnet flux-linkage Ψ_a can be calculated by magnetic flux ϕ and coil turns per phase N_c as follows:



(a) Quarter model



(b) Expanded figure of (a)



(c) 3-D model

Fig. 6. Structure of SPMMSM

Table 3. List of reluctances

Item	Symbol
Stator yoke	R_{SY}
Teeth	R_T
Air gap between teeth and magnet	R_{GI}
Permanent magnet	R_{PM}
Air gap both sides of magnet	R_{G2}
Rotor yoke	R_{RY}

$$\Psi_a = \sqrt{\frac{3}{2}} N_c \phi \dots \dots \dots \quad (19)$$

To use (19), magnetic flux ϕ and coil turns per phase N_c are as follows:

where

B_{SY} magnetic flux density of stator yoke

S_{SY} area of stator yoke ($= W_{SY} L_L$)

u winding space factor

S_{slot} area of slot

S_{wire} area of conducting wire

N_{slot} number of slot

Using (19), (20), (21), and stack length L_L , stator yoke

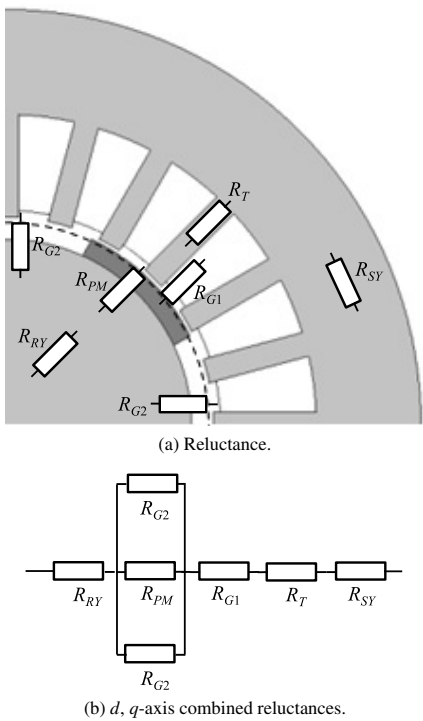


Fig. 7. Magnetic equivalent circuit

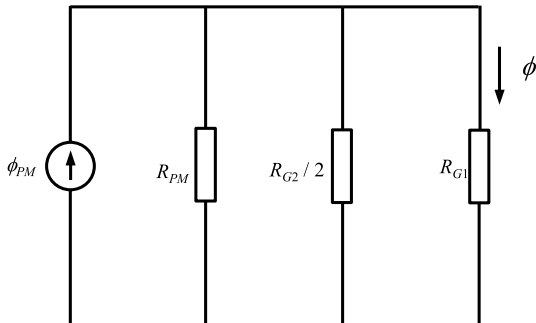


Fig. 8. Magnetic circuit from permeance model

width W_{SY} is calculated. Here, magnet flux-linkage Ψ_a given from the selection of motor parameters is used.

4.3 Inductance From Fig. 7, the sum of d -axis reluctance R_d is obtained as follows:

$$R_d = R_{SY} + R_T + R_{G1} + R_{PMG2} + R_{RY} \dots \dots \dots (22)$$

where

$$R_{PMG2} = R_{PM}R_{G2}/(2R_{PM} + R_{G1})$$

From (22), d -axis inductance L_d is as follows:

$$L_d = \frac{3N_c^2}{8R_d} \dots \dots \dots (23)$$

4.4 Magnetomotive Force The magnetic circuit from permanent magnet is shown in Fig. 8. In Fig. 8, only reluctances of R_{G1} , R_{G2} and R_{PM} are considered in order to constitute a simplified magnetic circuit. From Fig. 8, the equation of magnet flux ϕ_{PM} is given as follows:

$$\begin{aligned} \phi_{PM} &= \phi \left(\frac{1}{R_{PM}} + \frac{1}{R_{G1}} + \frac{1}{R_{G2}} \right) \div \frac{1}{R_{G1}} \\ &= B_{SY}S_{SY} \left(\frac{1}{R_{PM}} + \frac{1}{R_{G1}} + \frac{1}{R_{G2}} \right) \times R_{G1} \dots \dots \dots (24) \end{aligned}$$

Table 4. Parameters decided by motor designer

Item (Unit)	Value
Stator diameter D_s (mm)	124
Air gap length L_G (mm)	1.0
Numbers of teeth N_t	24
Cross-sectional area of the conducting wire S_{wire} (mm^2)	0.632
Space factor u	0.5
Relative permeability of electrical sheet μ_r	1000
Magnetic flux density of stator yoke B_{SY} (T)	0.85
$a (= D_r / L_L)$	1.5
$b (= D_r / D_s)$	0.5
$c (= W_T / W_{SY})$	0.5
Coercive force H_{cb} (kA/m)	900

Table 5. Result of structure parameters

Item (Unit)	Value	
Model	SPM-1	SPM-2
Selected motor parameters	MPP 1	MPP 2
Stator diameter D_s (mm)	124	
Airgap length L_G (mm)	1.0	
Rotor diameter D_r (mm)	62	
Stack length L_L (mm)	41.3	
Stator yoke width W_{SY} (mm)	12.8	
Teeth width W_T (mm)	6.4	
Magnet length L_{PM} (mm)	5.23	3.85
Magnet width W_{PM} (mm)	23.96	25.63

By using (24), the magnetomotive force F_{PM} is as follows:

$$F_{PM} = R_{PM}\phi_{PM} \dots \dots \dots (25)$$

By using the magnet coercive force H_{cb} , magnetomotive force F_{PM} is also given as follows:

$$F_{PM} = H_{cb}L_{PM} \dots \dots \dots (26)$$

From (25) and (26), the following equation is obtained:

$$R_{PM}\phi_{PM} = H_{cb}L_{PM} \dots \dots \dots (27)$$

From (23), (27) and $R_{PM} = L_{PM}/\mu_0 W_{PM} L_L$, magnet length L_{PM} and magnet width W_{PM} are obtained. The calculation of magnet length L_{PM} and magnet width W_{PM} uses d -axis inductance L_d obtained from the selection of motor parameters.

4.5 Design of Motor Structure Parameters The motor parameters in this design are shown in Table 4. The motor parameters are decided by a designer who design SPMSM by using the design assist system and the demanded specifications in advance. The values of the parameters in Table 4 are used. Generally, it is considered that the following dimensional ratios are suitable in the design of a high efficient motor⁽⁸⁾⁽⁹⁾. The ratio $a (= D_r / L_L)$ is about 1.5. The ratio $b (= D_r / D_s)$ is about 0.5 to 0.6. The ratio $c (= W_T / W_{SY})$ is about 0.5 to 0.6. In this paper, each value was selected within the above-mentioned suitable range.

The designed results are shown in Table 5. Two designed

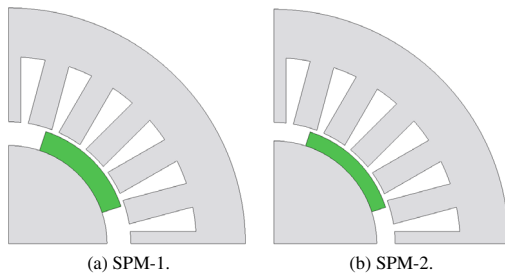


Fig. 9. Designed models

Table 6. Analysis condition

Item (Unit)	Value or Grade
Armature current limit I_{am} (A)	20
Induced voltage limit V_{om} (V)	100
Electrical steel sheet	50H470
Magnet	NMX-39EH (60°C)
Number of elements in mesh	about 23000

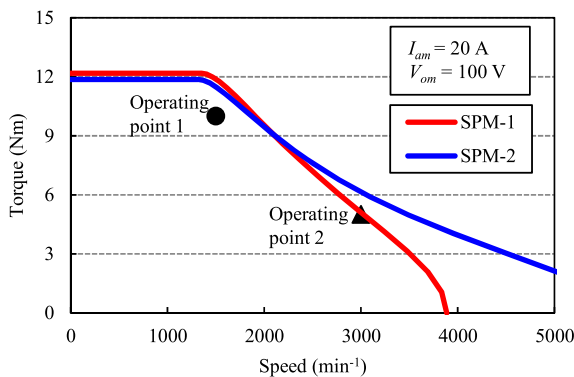


Fig. 10. Torque vs. speed characteristics of designed models

models are shown in Fig. 9. In the proposed design method, Ψ_a given by (19) is mainly used for stator design and L_a given by (23) is mainly used for rotor design. Therefore, the same stator was designed in SPM-1 and SPM-2 because Ψ_a is the same as shown in Table 2. On the other hand, the smaller the distance between the stator inner diameter and the rotor core outer diameter, the smaller the reluctance R_d , and as a result L_a increases. Therefore, it is thought that the magnet length of SPM-2 designed based on MPP-2 with larger L_a became smaller than that of SPM-1 designed based on MPP-1 with smaller L_a .

5. Analysis Result of Designed Model

To confirm that the designed models satisfy the demanded output characteristics, these models are analyzed by 2-D finite element method (FEM). The analysis condition is shown in Table 6. The torque-speed characteristics for the designed models are shown in Fig. 10. In Fig. 10, it is shown that the models satisfy the demanded output characteristics.

The values of magnet flux-linkage Ψ_a and inductance L_a of the designed motors, which were calculated by FEM, together with the selected motor parameters (the same values in Table 2) are shown in Table 7. The parameters of the designed motor are 10 to 20% larger than the selected motor parameters. The reason for this is that the calculation of mo-

Table 7. Selected motor parameters and designed motor parameters

Item (Unit)	MPP-1	SPM-1	MPP-2	SPM-2
Ψ_a (Wb)	0.252	0.304	0.252	0.297
L_a (mH)	7.5	8.92	9.5	10.4

tor structure parameters proposed in this paper is based on a simple magnetic equivalent circuit, the values of μ_s and B_{sy} used in designing were maybe different from the values of the designed motor. The appropriate setting of these parameters is a future task.

The characteristics of Figs. 10 and 4 appear to be somewhat different. The reason for this is that the parameters of the designed motor are different from the selected motor parameters as shown in Table 7. In the designed motor, the maximum torque was increased due to the increase in Ψ_a , and the torque at high speeds (in the flux-weakening control region) became lower as Ψ_a and L_a increased.

6. Conclusions

This paper proposes and describes a design assist system of the PMSM. This proposed system uses motor parameters that satisfy the demanded output characteristics, and is applied to the design of SPMSM. The motor structure parameters are calculated from the motor parameters and the restriction of motor size by using the magnetic equivalent circuit. The results of 2-D FEM analyses confirm that the SPMSMs designed by the proposed system satisfy the demanded output characteristics and the motor size. Therefore, the effectiveness of this proposed system is shown.

Acknowledgment

This work was supported by JSPS KAKENHI Grant Number JP23560335.

References

- (1) S. Morimoto, Y. Asano, T. Kosaka, and Y. Enomoto: "Recent Technical Trends in PMSM", in Proc. IPEC-2014, pp.1997–2003 (2014)
- (2) G. Pellegrino, A. Vagati, and P. Guglielmi: "Design Tradeoffs Between Constant Power Speed Range, Uncontrolled Generator Operation, and Rated Current of IPM Motor Drives", *IEEE Trans. Ind. Appl.*, Vol.47, No.5, pp.1995–2003 (2011)
- (3) N. Bernard, F. Martin, and M. E. Zaim: "Design Methology of a Permanent Magnet Synchronous Machine for a Screwdriver Application", *IEEE Trans. Energy. Convers.*, Vol.27, No.3, pp.624–633 (2012)
- (4) T. Yamada and K. Akatsu: "Automatic Design Method Considering the Frequently Used Area of a PMSM for an HEV", in Proc. ICEMS-2012 (2012)
- (5) N. Limsuwan, T. Fukushige, K. Akatsu, and R.D. Lorenz: "Design Methodology for Variable-Flux, Flux-Intensifying Interior Permanent Magnet Machines for an Electric-Vehicle-Class Inverter Rating", in Proc. ECCE-2013, pp.1547–1554 (2013)
- (6) B. Boazzo, G. Pellegrino, and A. Vagati: "Multipolar SPM Machines for Direct-Drive Application: A General Design Approach", *IEEE Trans. Ind. Appl.*, Vol.50, No.1, pp.327–337 (2014)
- (7) H.W. Lee, K.D. Lee, W.H. Kim, I.S. Jang, M.J. Kim, J.J. Lee, and J. Lee: "Parameters Design of IPMSM With Concentrated Winding Considering Partial Magnetic Saturation", *IEEE Trans. Magn.*, Vol.47, No.10, pp.3653–3656 (2011)
- (8) J-MAG motor design study group: "Introduction to Permanent Magnet Synchronous Motor Design", JSOL Corp. (2015) (in Japanese)
- (9) X. Ning, M. Sanada, and S. Morimoto: "Investigation of Design Parameters on Permanent Magnet Motors for HEV Applications", in Proc. ICEMS-2009, DS2G06_05 (2009)

Kenta Yamano (Student Member) received the B.E. and M.E. degrees from Osaka Prefecture University, Sakai, Japan, in 2015 and 2017, respectively. He was involved in the study on the design of permanent magnet synchronous motors at Osaka Prefecture University. He is currently with OBAYASHI CORPORATION, Tokyo, Japan.



Shigeo Morimoto (Senior Member) received the B.E., M.E., and Ph.D. degrees from Osaka Prefecture University, Sakai, Japan, in 1982, 1984, and 1990, respectively. In 1984, he joined Mitsubishi Electric Corporation, Tokyo, Japan. Since 1988, he has been with the Graduate School of Engineering, Osaka Prefecture University, where he is currently a Professor. His main areas of research interest are permanent magnet synchronous machines, reluctance machines and their control systems. Dr. Morimoto is a member of the IEEE, the Society of Instrument and Control Engineers of Japan, the Institute of Systems, Control and Information Engineers, and the Japan Institute of Power Electronics.



Masayuki Sanada (Senior Member) received the B.E., M.E., and Ph.D. degrees from Osaka Prefecture University, Sakai, Japan, in 1989, 1991, and 1994, respectively. Since 1994, he has been with the Graduate School of Engineering, Osaka Prefecture University, where he is currently an Associate Professor. His main areas of research interest are permanent-magnet motors for direct-drive applications, their control systems, and magnetic field analysis. Dr. Sanada is a member of the IEEE, the Japan Institute of Power Electronics, and the Japan Society of Applied Electromagnetics and Mechanics.

Yukinori Inoue (Member) received the B.E., M.E., and Ph.D. degrees from Osaka Prefecture University, Sakai, Japan, in 2005, 2007, and 2010, respectively. Since 2010, he has been with the Graduate School of Engineering, Osaka Prefecture University, where he is currently an Associate Professor. His research interests include control of electrical drives, in particular, the direct torque control of permanent magnet synchronous motors and position sensorless control of these motors. Dr. Inoue is a member of the IEEE and the Japan Institute of Power Electronics.